

Measurement of Coherent π^+ Production in Low Energy Neutrino-Carbon Scattering

K. Abe,⁴⁷ C. Andreopoulos,^{45,26} M. Antonova,²¹ S. Aoki,²³ A. Ariga,¹ S. Assylbekov,⁷ D. Autiero,²⁸ S. Ban,²⁴ M. Barbi,³⁹ G. J. Barker,⁵⁵ G. Barr,³⁵ P. Bartet-Friburg,³⁶ M. Batkiewicz,¹² F. Bay,¹⁰ V. Berardi,¹⁷ S. Berkman,³ S. Bhadra,⁵⁹ A. Blondel,¹¹ S. Bolognesi,⁵ S. Bordini,¹⁴ S. B. Boyd,⁵⁵ D. Brailsford,^{25,16} A. Bravar,¹¹ C. Bronner,²² M. Buizza Avanzini,⁹ R. G. Calland,²² T. Campbell,⁷ S. Cao,²⁴ J. Caravaca Rodríguez,¹⁴ S. L. Cartwright,⁴³ R. Castillo,¹⁴ M. G. Catanesi,¹⁷ A. Cervera,¹⁵ D. Cherdack,⁷ N. Chikuma,⁴⁶ G. Christodoulou,²⁶ A. Clifton,⁷ J. Coleman,²⁶ G. Collazuol,¹⁹ D. Coplowe,³⁵ L. Cremonesi,³⁸ A. Dabrowska,¹² G. De Rosa,¹⁸ T. Dealtry,²⁵ P. F. Denner,⁵⁵ S. R. Dennis,²⁶ C. Densham,⁴⁵ D. Dewhurst,³⁵ F. Di Lodovico,³⁸ S. Di Luise,¹⁰ S. Dolan,³⁵ O. Drapier,⁹ K. E. Duffy,³⁵ J. Dumarchez,³⁶ S. Dytman,³⁷ M. Dziewiecki,⁵⁴ S. Emery-Schrenk,⁵ A. Ereditato,¹ T. Feusels,³ A. J. Finch,²⁵ G. A. Fiorentini,⁵⁹ M. Friend,^{13,†} Y. Fujii,^{13,†} D. Fukuda,³³ Y. Fukuda,³⁰ A. P. Furmanski,⁵⁵ V. Galymov,²⁸ A. Garcia,¹⁴ S. G. Giffin,³⁹ C. Giganti,³⁶ F. Gizzarelli,⁵ M. Gonin,⁹ N. Grant,²⁵ D. R. Hadley,⁵⁵ L. Haegel,¹¹ M. D. Haigh,⁵⁵ P. Hamilton,¹⁶ D. Hansen,³⁷ J. Harada,³⁴ T. Hara,²³ M. Hartz,^{22,51} T. Hasegawa,^{13,†} N. C. Hastings,³⁹ T. Hayashino,²⁴ Y. Hayato,^{47,22} R. L. Helmer,⁵¹ M. Hierholzer,¹ A. Hillairet,⁵² A. Himmel,⁸ T. Hiraki,²⁴ S. Hirota,²⁴ M. Hogan,⁷ J. Holeczek,⁴⁴ S. Horikawa,¹⁰ F. Hosomi,⁴⁶ K. Huang,²⁴ A. K. Ichikawa,²⁴ K. Ieki,²⁴ M. Ikeda,⁴⁷ J. Imber,⁹ J. Insler,²⁷ R. A. Intonti,¹⁷ T. J. Irvine,⁴⁸ T. Ishida,^{13,†} T. Ishii,^{13,†} E. Iwai,¹³ K. Iwamoto,⁴⁰ A. Izmaylov,^{15,21} A. Jacob,³⁵ B. Jamieson,⁵⁷ M. Jiang,²⁴ S. Johnson,⁶ J. H. Jo,³² P. Jonsson,¹⁶ C. K. Jung,^{32,‡} M. Kabirnezhad,³¹ A. C. Kaboth,^{41,45} T. Kajita,^{48,‡} H. Kakuno,⁴⁹ J. Kameda,⁴⁷ D. Karlen,^{52,51} I. Karpikov,²¹ T. Katori,³⁸ E. Kearns,^{2,22,‡} M. Khabibullin,²¹ A. Khotjantsev,²¹ D. Kielczewska,^{53,*} T. Kikawa,²⁴ H. Kim,³⁴ J. Kim,³ S. King,³⁸ J. Kisiel,⁴⁴ A. Knight,⁵⁵ A. Knox,²⁵ T. Kobayashi,^{13,†} L. Koch,⁴² T. Koga,⁴⁶ A. Konaka,⁵¹ K. Kondo,²⁴ A. Kopylov,²¹ L. L. Kormos,²⁵ A. Korzenev,¹¹ Y. Koshio,^{33,‡} W. Kropp,⁴ Y. Kudenko,^{21,8} R. Kurjata,⁵⁴ T. Kutter,²⁷ J. Lagoda,³¹ I. Lamont,²⁵ E. Larkin,⁵⁵ P. Lasorak,^{38,38} M. Laveder,¹⁹ M. Lawe,²⁵ M. Lazos,²⁶ T. Lindner,⁵¹ Z. J. Liptak,⁶ R. P. Litchfield,¹⁶ X. Li,³² A. Longhin,¹⁹ J. P. Lopez,⁶ L. Ludovici,²⁰ X. Lu,³⁵ L. Magaletti,¹⁷ K. Mahn,²⁹ M. Malek,⁴³ S. Manly,⁴⁰ A. D. Marino,⁶ J. Marteau,²⁸ J. F. Martin,⁵⁰ P. Martins,³⁸ S. Martynenko,³² T. Maruyama,^{13,†} V. Matveev,²¹ K. Mavrokoridis,²⁶ W. Y. Ma,¹⁶ E. Mazzucato,⁵ M. McCarthy,⁵⁹ N. McCauley,²⁶ K. S. McFarland,⁴⁰ C. McGrew,³² A. Mefodiev,²¹ C. Metelko,²⁶ M. Mezzetto,¹⁹ P. Mijakowski,³¹ A. Minamino,²⁴ O. Mineev,²¹ S. Mine,⁴ A. Missert,⁶ M. Miura,^{47,‡} S. Moriyama,^{47,‡} Th. A. Mueller,⁹ S. Murphy,¹⁰ J. Myslik,⁵² T. Nakadaira,^{13,†} M. Nakahata,^{47,22} K. G. Nakamura,²⁴ K. Nakamura,^{22,13,†} K. D. Nakamura,²⁴ S. Nakayama,^{47,‡} T. Nakaya,^{24,22} K. Nakayoshi,^{13,‡} C. Nantais,³ C. Nielsen,³ M. Nirkko,¹ K. Nishikawa,^{13,†} Y. Nishimura,⁴⁸ P. Novella,¹⁵ J. Nowak,²⁵ H. M. O’Keeffe,²⁵ R. Ohta,^{13,†} K. Okumura,^{48,22} T. Okusawa,³⁴ W. Oryszczak,⁵³ S. M. Oser,³ T. Ovsyannikova,²¹ R. A. Owen,³⁸ Y. Oyama,^{13,†} V. Palladino,¹⁸ J. L. Palomino,³² V. Paolone,³⁷ N. D. Patel,²⁴ M. Pavin,³⁶ D. Payne,²⁶ J. D. Perkin,⁴³ Y. Petrov,³ L. Pickard,⁴³ L. Pickering,¹⁶ E. S. Pinzon Guerra,⁵⁹ C. Pistillo,¹ B. Popov,^{36,||} M. Posiadala-Zezula,⁵³ J.-M. Poutissou,⁵¹ R. Poutissou,⁵¹ P. Przewlocki,³¹ B. Quilain,²⁴ T. Radermacher,⁴² E. Radicioni,¹⁷ P. N. Ratoff,²⁵ M. Ravonel,¹¹ M. A. M. Rayner,¹¹ A. Redij,¹ E. Reinherz-Aronis,⁷ C. Riccio,¹⁸ P. Rojas,⁷ E. Rondio,³¹ S. Roth,⁴² A. Rubbia,¹⁰ A. Rychter,⁵⁴ R. Sacco,³⁸ K. Sakashita,^{13,†} F. Sánchez,¹⁴ F. Sato,¹³ E. Scantamburlo,¹¹ K. Scholberg,^{8,‡} S. Schoppmann,⁴² J. Schwehr,⁷ M. Scott,⁵¹ Y. Seiya,³⁴ T. Sekiguchi,^{13,†} H. Sekiya,^{47,22,‡} D. Sgalaberna,¹¹ R. Shah,^{45,35} A. Shaikhiev,²¹ F. Shaker,⁵⁷ D. Shaw,²⁵ M. Shiozawa,^{47,22} T. Shirahige,³³ S. Short,³⁸ M. Smy,⁴ J. T. Sobczyk,⁵⁸ H. Sobel,^{4,22} M. Sorel,¹⁵ L. Southwell,²⁵ P. Stamoulis,¹⁵ J. Steinmann,⁴² T. Stewart,⁴⁵ P. Stowell,⁴³ Y. Suda,⁴⁶ S. Suvorov,²¹ A. Suzuki,²³ K. Suzuki,²⁴ S. Y. Suzuki,^{13,†} Y. Suzuki,²² R. Tacik,^{39,51} M. Tada,^{13,†} S. Takahashi,²⁴ A. Takeda,⁴⁷ Y. Takeuchi,^{23,22} H. K. Tanaka,^{47,‡} H. A. Tanaka,^{50,51,¶} D. Terhorst,⁴² R. Terri,³⁸ T. Thakore,²⁷ L. F. Thompson,⁴³ S. Tobayama,³ W. Toki,⁷ T. Tomura,⁴⁷ C. Touramanis,²⁶ T. Tsukamoto,^{13,†} M. Tzanov,²⁷ Y. Uchida,¹⁶ A. Vacheret,³⁵ M. Vagins,^{22,4} Z. Vallari,³² G. Vasseur,⁵ T. Wachala,¹² K. Wakamatsu,³⁴ C. W. Walter,^{8,‡} D. Wark,^{45,35} W. Warzycha,⁵³ M. O. Wascko,^{16,13} A. Weber,^{45,35} R. Wendell,^{24,‡} R. J. Wilkes,⁵⁶ M. J. Wilking,³² C. Wilkinson,¹ J. R. Wilson,³⁸ R. J. Wilson,⁷ Y. Yamada,^{13,†} K. Yamamoto,³⁴ M. Yamamoto,²⁴ C. Yanagisawa,^{32,**} T. Yano,²³ S. Yen,⁵¹ N. Yershov,²¹ M. Yokoyama,^{46,‡} J. Yoo,²⁷ K. Yoshida,²⁴ T. Yuan,⁶ M. Yu,⁵⁹ A. Zalewska,¹² J. Zalipska,³¹ L. Zambelli,^{13,†} K. Zaremba,⁵⁴ M. Ziembicki,⁵⁴ E. D. Zimmerman,⁶ M. Zito,⁵ and J. Żmuda⁵⁸

(The T2K Collaboration)

¹University of Bern, Albert Einstein Center for Fundamental Physics, Laboratory for High Energy Physics (LHEP), Bern, Switzerland

²Department of Physics, Boston University, Boston, Massachusetts, USA

³Department of Physics and Astronomy, University of British Columbia, Vancouver, British Columbia, Canada

⁴Department of Physics and Astronomy, University of California, Irvine, Irvine, California, USA

- ⁵IRFU, CEA Saclay, Gif-sur-Yvette, France
- ⁶Department of Physics, University of Colorado at Boulder, Boulder, Colorado, USA
- ⁷Department of Physics, Colorado State University, Fort Collins, Colorado, USA
- ⁸Department of Physics, Duke University, Durham, North Carolina, USA
- ⁹Ecole Polytechnique, IN2P3-CNRS, Laboratoire Leprince-Ringuet, Palaiseau, France
- ¹⁰ETH Zurich, Institute for Particle Physics, Zurich, Switzerland
- ¹¹University of Geneva, Section de Physique, DPNC, Geneva, Switzerland
- ¹²H. Niewodniczanski Institute of Nuclear Physics PAN, Cracow, Poland
- ¹³High Energy Accelerator Research Organization (KEK), Tsukuba, Ibaraki, Japan
- ¹⁴Institut de Física d'Altes Energies (IFAE), The Barcelona Institute of Science and Technology, Campus UAB, Bellaterra (Barcelona), Spain
- ¹⁵IFIC (CSIC & University of Valencia), Valencia, Spain
- ¹⁶Department of Physics, Imperial College London, London, United Kingdom
- ¹⁷INFN Sezione di Bari and Università e Politecnico di Bari, Dipartimento Interuniversitario di Fisica, Bari, Italy
- ¹⁸Dipartimento di Fisica, INFN Sezione di Napoli and Università di Napoli, Napoli, Italy
- ¹⁹Dipartimento di Fisica, INFN Sezione di Padova and Università di Padova, Padova, Italy
- ²⁰INFN Sezione di Roma and Università di Roma "La Sapienza", Roma, Italy
- ²¹Institute for Nuclear Research of the Russian Academy of Sciences, Moscow, Russia
- ²²Kavli Institute for the Physics and Mathematics of the Universe (WPI), The University of Tokyo Institutes for Advanced Study, University of Tokyo, Kashiwa, Chiba, Japan
- ²³Kobe University, Kobe, Japan
- ²⁴Department of Physics, Kyoto University, Kyoto, Japan
- ²⁵Physics Department, Lancaster University, Lancaster, United Kingdom
- ²⁶Department of Physics, University of Liverpool, Liverpool, United Kingdom
- ²⁷Department of Physics and Astronomy, Louisiana State University, Baton Rouge, Louisiana, USA
- ²⁸Université de Lyon, Université Claude Bernard Lyon 1, IPN Lyon (IN2P3), Villeurbanne, France
- ²⁹Department of Physics and Astronomy, Michigan State University, East Lansing, Michigan, USA
- ³⁰Department of Physics, Miyagi University of Education, Sendai, Japan
- ³¹National Centre for Nuclear Research, Warsaw, Poland
- ³²Department of Physics and Astronomy, State University of New York at Stony Brook, Stony Brook, New York, USA
- ³³Department of Physics, Okayama University, Okayama, Japan
- ³⁴Department of Physics, Osaka City University, Osaka, Japan
- ³⁵Department of Physics, Oxford University, Oxford, United Kingdom
- ³⁶UPMC, Université Paris Diderot, CNRS/IN2P3, Laboratoire de Physique Nucléaire et de Hautes Energies (LPNHE), Paris, France
- ³⁷Department of Physics and Astronomy, University of Pittsburgh, Pittsburgh, Pennsylvania, USA
- ³⁸School of Physics and Astronomy, Queen Mary University of London, London, United Kingdom
- ³⁹Department of Physics, University of Regina, Regina, Saskatchewan, Canada
- ⁴⁰Department of Physics and Astronomy, University of Rochester, Rochester, New York, USA
- ⁴¹Department of Physics, Royal Holloway University of London, Egham, Surrey, United Kingdom
- ⁴²RWTH Aachen University, III. Physikalisches Institut, Aachen, Germany
- ⁴³Department of Physics and Astronomy, University of Sheffield, Sheffield, United Kingdom
- ⁴⁴Institute of Physics, University of Silesia, Katowice, Poland
- ⁴⁵STFC, Rutherford Appleton Laboratory, Harwell Oxford, and Daresbury Laboratory, Warrington, United Kingdom
- ⁴⁶Department of Physics, University of Tokyo, Tokyo, Japan
- ⁴⁷Institute for Cosmic Ray Research, University of Tokyo, Kamioka Observatory, Kamioka, Japan
- ⁴⁸Institute for Cosmic Ray Research, University of Tokyo, Research Center for Cosmic Neutrinos, Kashiwa, Japan
- ⁴⁹Tokyo Metropolitan University, Department of Physics, Tokyo, Japan
- ⁵⁰Department of Physics, University of Toronto, Toronto, Ontario, Canada
- ⁵¹TRIUMF, Vancouver, British Columbia, Canada
- ⁵²Department of Physics and Astronomy, University of Victoria, Victoria, British Columbia, Canada
- ⁵³Faculty of Physics, University of Warsaw, Warsaw, Poland
- ⁵⁴Institute of Radioelectronics, Warsaw University of Technology, Warsaw, Poland
- ⁵⁵Department of Physics, University of Warwick, Coventry, United Kingdom
- ⁵⁶Department of Physics, University of Washington, Seattle, Washington, USA
- ⁵⁷Department of Physics, University of Winnipeg, Winnipeg, Manitoba, Canada
- ⁵⁸Faculty of Physics and Astronomy, Wrocław University, Wrocław, Poland
- ⁵⁹Department of Physics and Astronomy, York University, Toronto, Ontario, Canada

(Received 15 April 2016; revised manuscript received 26 September 2016; published 4 November 2016)

We report the first measurement of the flux-averaged cross section for charged current coherent π^+ production on carbon for neutrino energies less than 1.5 GeV, and with a restriction on the final state phase space volume in the T2K near detector, ND280. Comparisons are made with predictions from the Rein-Sehgal coherent production model and the model by Alvarez-Ruso *et al.*, the latter representing the first implementation of an instance of the new class of microscopic coherent models in a neutrino interaction Monte Carlo event generator. We observe a clear event excess above background, disagreeing with the null results reported by K2K and SciBooNE in a similar neutrino energy region. The measured flux-averaged cross sections are below those predicted by both the Rein-Sehgal and Alvarez-Ruso *et al.* models.

DOI: 10.1103/PhysRevLett.117.192501

Introduction.—Charged current coherent pion production in neutrino-nucleus scattering, $\nu_\mu + A \rightarrow \mu^- + \pi^+ + A$, is a process in which the neutrino scatters coherently from an entire nucleus, leaving the nucleus unchanged. No quantum numbers are exchanged and there is little four-momentum transfer to any nucleon. Because of these restrictions the outgoing lepton and pion are aligned with the beam direction and no other hadrons are produced.

Two classes of models have been developed to describe this process. The first class uses Adler's theorem [1] to relate the coherent scattering cross section at $Q^2 = -q^2 = -(p_\nu - p_\mu)^2 = 0$ with the pion-nucleus elastic scattering cross section. Described by the diagram shown in Fig. 1(a), the differential cross section is

$$\left. \frac{d\sigma_{coh}}{dQ^2 dy d|t|} \right|_{Q^2=0} = \frac{G_F^2}{2\pi^2} f_\pi^2 \frac{1-y}{y} \frac{d\sigma(\pi A \rightarrow \pi A)}{d|t|}, \quad (1)$$

where $y = E_\pi/E_\nu$ with E_π and E_ν being the energy of the pion and neutrino, respectively; f_π is the pion decay constant and $|t| = |(q - p_\pi)|^2$ is the magnitude of the square of the four-momentum transferred by the exchange boson to the nucleus. Different models [2–5] choose different methods for extension to $Q^2 > 0$ and implementations of the πA elastic scattering cross section. The validity of these models below neutrino energies of roughly 2 GeV is limited [6–9].

The second class, known as the microscopic models, was developed specifically for neutrino energies less than 2 GeV [8,10–13]. These models are based on the single nucleon process $\nu_l N \rightarrow l^- N \pi^+$, which is dominated by Δ production at low energies as shown in the right diagram in Fig. 1(b). The total cross section is derived from the coherent sum of the contribution of all nucleons within the individual nuclei. Effects of the nuclear medium on the Δ and on the pion wave function are taken into account. These models have not been tested against data. Only recently has one instance of this class, the model from Alvarez-Ruso *et al.* [11], been implemented in a neutrino event generator.

The charged current coherent production cross section has been measured at neutrino energies above 7 GeV by several experiments [14–18] and has been found to agree

with the standard coherent model developed by Rein and Sehgal. More recent model dependent searches by K2K [19] and SciBooNE [20] at neutrino energies of 0.5–2 GeV suffer from low statistics and reported null results. Recently the MINER ν A experiment published a measurement of this cross section for neutrino energies between 1.5 and 20.0 GeV [21].

This Letter presents the first measurement of the charged current coherent pion production cross section below a neutrino energy of 1.5 GeV. The analysis conducts a model independent search for an excess of events at low $|t|$. The flux-averaged charged current coherent pion production cross section is presented for two regions of the final state phase space. The restricted final state phase space region is limited to $p_{\mu,\pi} > 0.18$ GeV/c, $\theta_{\mu,\pi} < 70^\circ$, which removes areas of low detector acceptance, and $p_\pi < 1.6$ GeV/c, which removes an area outside the range of validity of the microscopic model. The angles of the muon and pion, $\theta_{\mu,\pi}$, are measured with respect to the average direction of the incoming neutrino beam.

The flux-averaged cross section for production to the complete phase space is also presented. In addition, for each choice of final state phase space coverage, we present results using two different models: the Rein-Sehgal model [6] as implemented in the GENIE 2.6.4 neutrino event generator (which uses a more sophisticated parametrization of the pion-nucleus elastic scattering than outlined in the original Rein-Sehgal paper [22]) and an implementation of the microscopic model constructed by Alvarez-Ruso *et al.* [11]. Previous null results [19,20] used the Rein-Sehgal coherent model to devise and tune kinematic cuts and were, thus, not model independent.

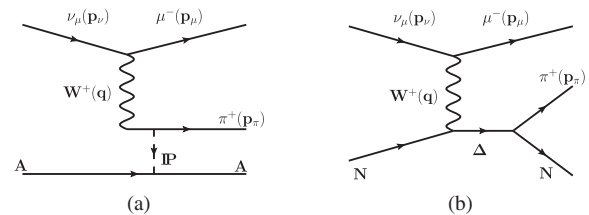


FIG. 1. (a) Diagram for coherent charged pion production model based on Adler's theorem. The \mathbb{P} represents the transfer of a Pomeron to the nuclear system. (b) Dominant diagram for the microscopic class of coherent charged pion production models.

T2K experiment.—T2K [23] is an off-axis long-baseline neutrino oscillation experiment sited at the J-PARC facility in Tokai, Japan. A complete description of the experiment may be found in Ref. [23]. The experiment views an off-axis neutrino beam flux that is composed of 92.6% ν_μ with a peak ν_μ energy of 0.6 GeV. The neutrino beam is described in detail in Refs. [23] and [24]. The data used in this analysis correspond to 5.54×10^{20} protons on target.

ND280 [23] is the off-axis magnetized tracking near detector designed to measure interactions of both ν_μ and ν_e from the T2K beam before oscillations. The detector rests within the refurbished UA1/NOMAD magnet, which provides a magnetic field of 0.2 T, and is split into two regions: the upstream π^0 detector [25] and the tracker. The tracker region contains two plastic scintillator detectors [26] [fine grained detectors (FGDs)], used as targets for neutrino interactions, sandwiched between three argon-gas time projection chambers (TPCs) [27]. The first, most upstream, FGD (FGD1) only has layers of plastic (CH) scintillator bars while the second FGD (FGD2) also contains water layers. Surrounding these inner subdetectors is a set of electromagnetic calorimeters [28]. The magnet yokes are instrumented with scintillator-based side muon range detectors [29] to track high angle muons.

Neutrino interactions are simulated using the default GENIE 2.6.4 neutrino event generator package [5]. Quasielastic scattering is modeled using the Llewellyn-Smith [30] model with an axial mass, m_A , set to $0.99 \text{ GeV}/c^2$. The initial state nuclear model is the Bodek-Ritchie relativistic Fermi gas model with a Fermi momentum of $221 \text{ MeV}/c$, extended to include short range nucleon-nucleon correlations [31]. Inelastic single pion production from resonances is simulated using the Rein-Sehgal model [32]. Interference between the resonance states and lepton mass effects is ignored, although the effect of lepton masses on phase space boundaries is taken into account. Nonresonant pion production is modeled using an extension of the Bodek-Yang model [33] to low energies. Interference between the resonant and non-resonant interaction modes is not taken into account. The relative contributions were tuned by GENIE against available single pion production cross section data [5]. The transition to nonresonant inelastic scattering is simulated using the same Bodek-Yang model. Hadronization is described using the AGKY model [34]. Hadronic interactions in the nuclear medium are modeled using the INTRANUKE package [5].

Event selection.—This analysis uses neutrino interactions that have occurred in the scintillator target of FGD1. Charged particles in the final state are analyzed by the second TPC, which lies immediately downstream of FGD1. The first step is to select ν_μ charged current inclusive events in FGD1 using the event selection criteria reported in detail in Ref. [35]. Events passing this selection are in time with the beam and contain at least one negatively charged track in TPC2 consistent with a

minimally ionizing particle. The interaction vertex is defined to be the most upstream point of the muon candidate track. This must lie within the fiducial volume of FGD1, which excludes the two most upstream and downstream layers, and the outermost five bars in each layer. All previously published results do not use vertex activity and do not impose such a constraint on the downstream fiducial boundary. The resulting fiducial region contains 0.74 tonnes of carbon [36].

An event sample with an enhanced coherent pion component is then selected by requiring a second, positively charged, track originating from the interaction vertex. This second track is required to have a dE/dx profile consistent with a muon or pion traversing the TPC. Cuts to enforce this requirement remove proton tracks such that they make up less than 3% of the selected pion candidates.

Charged current coherent pion production leaves the nuclear target unchanged and in its ground state. Hence the only particles exiting the interaction are a charged lepton and an oppositely charged pion. Events with additional energy deposited around the vertex are removed by a cut on the vertex activity (VA), which is defined to be the sum of all energy deposits within a cubic volume with side length 5 cm centered on the vertex. No attempt is made to estimate and subtract the energy deposited by the muon and pion within this region. Simulated coherent events typically deposit 220 photon equivalent units (PEU [37]) with an rms spread of 40 PEU. Sixty percent of the predicted background is removed by requiring the VA in the event to be less than 300 PEU with no loss of predicted signal.

Analysis strategy.—In the models based on Adler's theorem, coherent interactions are characterized by the low transfer of four-momentum to the nucleus. Referring to the diagram in Fig. 1(a), this quantity is defined to be

$$|t| = |(q - p_\pi)^2| = \left(\sum_{i=\mu,\pi} (E_i - p_i^L) \right)^2 + \left(\sum_{i=\mu,\pi} p_i^T \right)^2, \quad (2)$$

where the approximation that negligible energy is transferred to the nucleus has been made, and p^T and p^L are the transverse and longitudinal components of the particle's momentum with respect to the direction of the neutrino beam. The microscopic models also predict events clustering at low values of $|t|$. This experimental observable is well defined regardless of the class of model under consideration. This analysis searches for an excess of events above background at low $|t|$. No attempt is made to fit any particular model to the data.

Sources of systematic uncertainty.—The flux-averaged cross section is given by $\langle \sigma_{\text{coh}} \rangle = (N_{\text{sel}} - N_{bg}) / \Phi N_T \epsilon$, where N_{sel} is the number of selected events, N_{bg} is the estimated number of background events, ϵ is the coherent event selection efficiency, N_T is the number of target carbon nuclei, and Φ is the integrated T2K neutrino flux

incident on FGD1. The largest uncertainties on the flux-averaged cross section arise from the flux model, the background interaction model, the model for final state pion reinteractions within the detector, and the model for the VA. Estimates of the uncertainty on the coherent cross section are determined by varying model parameters within their uncertainties, and propagating the changes to the result.

The flux systematic uncertainty is evaluated by varying the shape and normalization of the T2K flux prediction [24]. The uncertainties in the parameters of the background cross section models are constrained by previous measurements as implemented in the default configuration of the GENIE generator [5,38]. The pion reinteraction uncertainty is evaluated by varying the total pion absorption and charge exchange cross sections within bounds defined by the difference between GEANT4 and published hadronic interaction data [39].

The VA uncertainty arises from two sources: the charge response of the FGD to energy deposition and the simulation of energy produced at the vertex in the charged current coherent π^+ background event sample. The former was studied by comparing the charge response of the FGD to protons stopping in the FGD fiducial volume in data and Monte Carlo calculations. The simulation was found to underestimate the average measured charge deposit by 10% and this was taken to be the systematic uncertainty in the FGD charge response.

The average VA of the simulated coherent background control sample was lower than that observed in the data. The issue of multinucleon knockout effects in neutrino scattering has recently received much attention (see, for example, [40,41]). Such effects would eject low momentum protons into the region around the vertex, increasing the average VA. Indeed, the simulated VA distribution can be made to agree better with background data by adding VA consistent with that deposited by a proton with kinetic energy distributed uniformly between 20 and 225 MeV to 25% of background events with a neutron target. The MINER ν A experiment reported a similar observation in a study of neutrino-nucleus quasielastic interactions [42,43]. The uncertainty in the vertex activity model was derived by switching this addition on and off. No correction is applied for this effect in deriving the cross section or significance of the signal. This is the dominant systematic uncertainty in the estimate of the background to the charged current coherent π^+ signal.

Background estimate.—The estimated number of background interactions is constrained by fits to the data. The event sample was divided into a signal enriched sample, with $|t| < 0.15$ (GeV) c^2 and VA < 300 PEU, and two side-band regions. The first side band is comprised of events that fail the VA cut [$|t| < 0.15$ (GeV) c^2 and VA > 300 PEU], while the second region contains events that fail the $|t|$ cut ($|t| > 0.15$ (GeV) c^2 and

VA < 300 PEU). The Monte Carlo predicts a $|t|$ resolution for signal events of less than 0.02 (GeV) c^2 . The signal enriched region was defined to include more than 99% of the coherent signal predicted by either model. Events in the side-band samples were then sorted into bins of reconstructed invariant mass, W . Template distributions of pion momenta were formed for each W bin and scale factors estimated by fitting the normalization of each W bin to the data. The variation in W was constrained by the covariance matrices encoding the effects of the variation in the systematic parameters described above.

The scale factors resulting from the fit to the side bands were constant at 89% over the full W -range. The prefit incoherent background prediction was thereby reduced from 88 events to 78 ± 18 . The fractional uncertainties in the background estimate from these sources of uncertainty are shown in Table I.

Results.—The distribution of $|t|$ for the data and the predicted background, both after the VA cut is applied, is shown in Fig. 2. There is a clear excess of events in the data at low $|t|$ that is consistent with a charged current coherent π^+ production signal, while the shape of the high $|t|$ region is consistent with the background prediction. The total number of events observed in the signal region in the data is 123. After background subtraction, the number of coherent events in the data is 45 ± 18 . The significance of observing such an excess of events is 2.2σ with a p value of 0.014.

The model dependent efficiency for selecting coherent events in the restricted phase space ($p_{\mu,\pi} > 0.18$ GeV/ c , $\theta_{\mu,\pi} < 70^\circ$ and $p_\pi < 1.6$ GeV/ c) is 38% (42%) if the Rein-Sehgal (Alvarez-Ruso *et al.*) model is used. The difference between efficiency arises from the effect of the particle identification criterion applied to differing pion kinematic distributions in the models. The cross section for scattering to the restricted phase space is $(3.2 \pm 0.8(\text{stat})_{-1.2}^{+1.3}(\text{sys})) \times 10^{-40}$ cm 2 / ^{12}C nucleus using the Rein-Sehgal model, and $(2.9 \pm 0.7(\text{stat})_{-1.1}^{+1.1}(\text{sys})) \times 10^{-40}$ cm 2 / ^{12}C nucleus using the model from Alvarez-Ruso *et al.* These should be compared to the predictions of 5.3×10^{-40} cm 2 / ^{12}C nucleus and

TABLE I. Summary of the fractional systematic uncertainties on the background estimate and on the phase space restricted charged current coherent flux-averaged cross section ($\langle \sigma_{\text{coh}}^{\text{rest}} \rangle$).

Systematic source	Fractional error on background	Fractional error on $\langle \sigma_{\text{coh}}^{\text{rest}} \rangle$
Flux model	0.05	0.10
Background model	0.14	0.25
Pion reinteractions	+0.05–0.01	+0.14–0.05
Vertex activity model	0.19	0.28
FGD charge scale	0.06	0.15

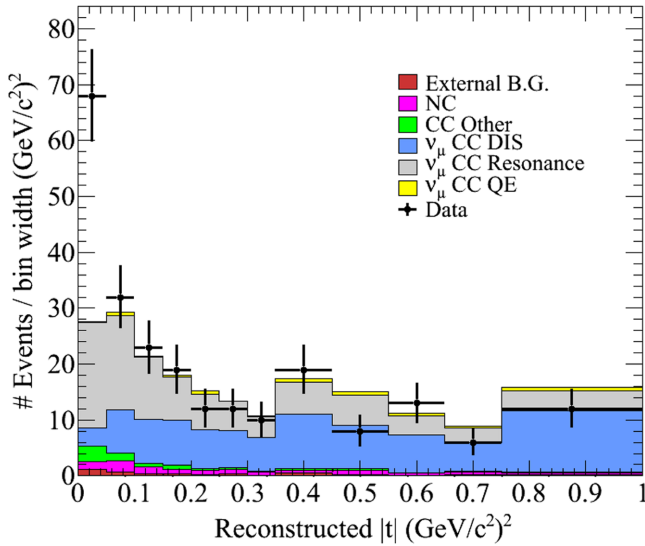


FIG. 2. The reconstructed $|t|$ distribution after the VA cut and the background tuning procedure have been applied. The errors on the data are statistical only, and the uncertainty on the tuned model is not shown. The model's prediction of the coherent contribution has been removed from the plot. The small external background component contains events that occur outside the FGD1 fiducial volume, such as interactions occurring in the surrounding magnet volume.

$4.5 \times 10^{-40} \text{ cm}^2/^{12}\text{C}$ nucleus from the models by Rein-Sehgal and Alvarez-Ruso *et al.*, respectively. The fractional uncertainty on these estimates from each of the main sources of systematic error is shown in Table I. There is no guidance for the uncertainty of the coherent models in the T2K neutrino energy regime and so we do not include a systematic uncertainty for the signal event selection

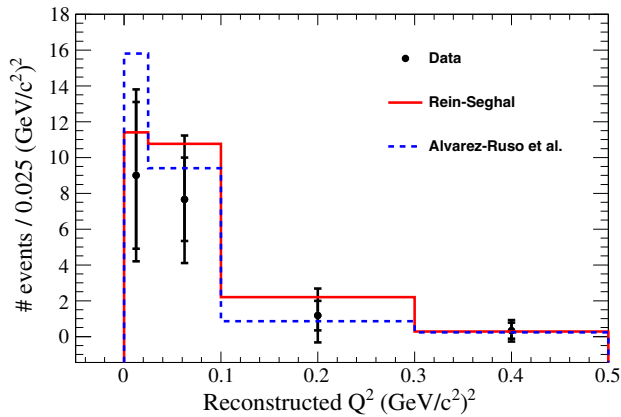


FIG. 3. The reconstructed Q^2 distribution after background subtraction. The inner error bars represent the statistical uncertainty on the data before background subtraction and the outer the total uncertainty that also includes systematic effects. Correlations between bins are not reflected in the uncertainty displayed on the figure. The last bin is an overflow bin, containing all events with reconstructed Q^2 greater than $0.3 \text{ (GeV/c}^2)^2$.

efficiency in the cross section measurement. Figure 3 shows the background subtracted reconstructed Q^2 distribution compared to the two models.

Total flux-averaged cross sections may be estimated by correcting these results by the fraction of the full phase space contained within the restricted phase space region predicted by the model. The total flux-averaged cross section is therefore inherently dependent on the signal model. The correction required for the two models is 1.20 for the Rein-Sehgal model and 1.17 for the Alvarez-Ruso *et al.* model, leading to the total flux-averaged charged current coherent scattering cross section of $(3.9 \pm 1.0(\text{stat})^{+1.5}(\text{sys})) \times 10^{-40} \text{ cm}^2/^{12}\text{C}$ nucleus for the Rein-Sehgal model and $(3.3 \pm 0.8(\text{stat})^{+1.3}(\text{sys})) \times 10^{-40} \text{ cm}^2/^{12}\text{C}$ nucleus in the context of the Alvarez-Ruso *et al.* model. These should be compared to the predictions of $6.4 \times 10^{-40} \text{ cm}^2/^{12}\text{C}$ nucleus and $5.3 \times 10^{-40} \text{ cm}^2/^{12}\text{C}$ nucleus from the Rein-Sehgal and Alvarez-Ruso *et al.* models, respectively.

It should be noted that T2K oscillation analyses utilize a version of the NEUT event generator that has undergone extensive tuning with non-T2K neutrino scattering data and then been fitted to T2K near detector data [44]. This predicts a total charged current coherent scattering flux-averaged cross section of $6.7 \times 10^{-40} \text{ cm}^2/^{12}\text{C}$ nucleus, consistent with the measurement reported here. By contrast, the standard untuned NEUT predicts a total charged current coherent scattering flux-averaged cross section of $15.3 \times 10^{-40} \text{ cm}^2/^{12}\text{C}$ nucleus. The discrepancy with GENIE arises from the differing implementations of the pion-nucleus cross section.

Conclusion.—T2K has made the first measurement of the cross section for charged current coherent production of a pion from carbon nuclei for neutrino energies less than 1.5 GeV . This has been presented both in the restricted final state phase space ($p_{\mu,\pi} > 0.18 \text{ GeV}/c$, $\theta_{\mu,\pi} < 70^\circ$ and $p_\pi < 1.6 \text{ GeV}/c$) and the total final state phase space. This result disagrees with the null results reported previously by the K2K [19] and SciBooNE [20] experiments. These measurements have been compared to the standard Rein-Sehgal model and, for the first time, an instance of the class of microscopic models. While T2K observes a clear excess above background the measured flux-averaged cross sections are below those predicted by both the Rein-Sehgal and the Alvarez-Ruso *et al.* models. The statistical precision is insufficient to distinguish between the models.

We thank the J-PARC staff for superb accelerator performance and the CERN NA61 Collaboration for providing valuable particle production data. We acknowledge the support of MEXT, Japan; NSERC (Grant No. SAPPJ-2014-00031), NRC and CFI, Canada; CEA and CNRS/IN2P3, France; DFG, Germany; INFN, Italy; National Science Centre (NCN), Poland; RSF, RFBR, and Ministry of Education and Science (MES), Russia; MINECO and European Regional Development (ERDF)

funds, Spain; Swiss National Science Foundation (SNSF) and State Secretariat for Education, Research and Innovation (SERI), Switzerland; STFC, UK; and DOE, USA. We also thank CERN for the UA1/NOMAD magnet, DESY for the HERA-B magnet mover system, NII for SINET4, the WestGrid and SciNet consortia in Compute Canada, and GridPP in the United Kingdom. In addition, participation of individual researchers and institutions has been further supported by funds from ERC (FP7), H2020 Grant No. RISE-GA644294-JENNIFER, EU; JSPS, Japan; Royal Society, UK; and the DOE Early Career program, USA.

*Deceased.

[†]Also at J-PARC, Tokai, Japan.

[‡]Also at Kavli IPMU (WPI), the University of Tokyo, Japan.

[§]Also at National Research Nuclear University “MEPhI” and Moscow Institute of Physics and Technology, Moscow, Russia.

^{||}Also at JINR, Dubna, Russia.

[¶]Also at Institute of Particle Physics, Canada.

**Also at BMCC/CUNY, Science Department, New York, New York, USA.

- [1] S. L. Adler, *Phys. Rev.* **135**, B963 (1964).
- [2] A. A. Belkov and B. Z. Kopeliovich, *Yad. Fiz.* **46**, 874 (1987) [*Sov. J. Nucl. Phys.* **46**, 499 (1987)].
- [3] C. Berger and L. M. Sehgal, *Phys. Rev. D* **79**, 053003 (2009).
- [4] E. A. Paschos and D. Schalla, *Phys. Rev. D* **80**, 033005 (2009).
- [5] C. Andreopoulos *et al.*, *Nucl. Instrum. Methods Phys. Res., Sect. A* **614**, 87 (2010).
- [6] D. Rein and L. M. Sehgal, *Nucl. Phys.* **B223**, 29 (1983).
- [7] E. Hernandez, J. Nieves, and M. J. VicenteVacas, *Phys. Rev. D* **80**, 013003 (2009).
- [8] E. Hernandez, J. Nieves, and M. Valverde, *Phys. Rev. D* **82**, 077303 (2010).
- [9] J. E. Amaro, E. Hernandez, J. Nieves, and M. Valverde, *Phys. Rev. D* **79**, 013002 (2009).
- [10] S. K. Singh, M. S. Athar, and S. Ahmad, *Phys. Rev. Lett.* **96**, 241801 (2006).
- [11] L. Alvarez-Ruso, L. S. Geng, S. Hirenzaki, and M. J. VicenteVacas, *Phys. Rev. C* **75**, 055501 (2007).
- [12] T. Leitner, U. Mosel, and S. Winkelmann, *Phys. Rev. C* **79**, 057601 (2009).
- [13] S. X. Nakamura, T. Sato, T. S. H. Lee, B. Szczerbinska, and K. Kubodera, *Phys. Rev. C* **81**, 035502 (2010).
- [14] P. P. Allport *et al.* (BEBC WA59 Collaboration), *Z. Phys. C* **43**, 523 (1989).
- [15] P. Vilain *et al.* (CHARM-II Collaboration), *Phys. Lett. B* **313**, 267 (1993).
- [16] H. J. Grabosch *et al.* (SKAT Collaboration), *Z. Phys. C* **31**, 203 (1986).
- [17] S. Willocq *et al.* (E632 Collaboration), *Phys. Rev. D* **47**, 2661 (1993).
- [18] R. Acciarri *et al.* (ArgoNeuT Collaboration), *Phys. Rev. Lett.* **113**, 261801 (2014); **114**, 039901 (2015).
- [19] M. Hasegawa *et al.* (K2K Collaboration), *Phys. Rev. Lett.* **95**, 252301 (2005).
- [20] K. Hiraide *et al.* (SciBooNE Collaboration), *Phys. Rev. D* **78**, 112004 (2008).
- [21] A. Higuera *et al.* (MINERvA Collaboration), *Phys. Rev. Lett.* **113**, 261802 (2014).
- [22] Note that the official version of GENIE 2.6.4 incorporates an error in the calculation of the pion-nucleus cross section. This error was fixed in GENIE versions 2.8.2 and beyond. The error has also been fixed for the version of 2.6.4 used in the current analysis.
- [23] K. Abe *et al.* (T2K Collaboration), *Nucl. Instrum. Methods Phys. Res., Sect. A* **659**, 106 (2011).
- [24] K. Abe *et al.* (T2K Collaboration), *Phys. Rev. D* **87**, 012001 (2013).
- [25] S. Assylbekov, G. Barr, B. E. Berger, H. Berns, D. Beznosko *et al.*, *Nucl. Instrum. Methods Phys. Res., Sect. A* **686**, 48 (2012).
- [26] P. A. Amaudruz *et al.* (T2K ND280 FGD Collaboration), *Nucl. Instrum. Methods Phys. Res., Sect. A* **696**, 1 (2012).
- [27] N. Abgrall *et al.* (T2K ND280 TPC Collaboration), *Nucl. Instrum. Methods Phys. Res., Sect. A* **637**, 25 (2011).
- [28] D. Allan *et al.* (T2K UK Collaboration), *J. Instrum.* **8**, P10019 (2013).
- [29] S. Aoki, G. Barr, M. Batkiewicz, J. Blocki, J. D. Brinson *et al.*, *Nucl. Instrum. Methods Phys. Res., Sect. A* **698**, 135 (2013).
- [30] C. H. Llewellyn-Smith, *Phys. Rep.* **3**, 261 (1972).
- [31] A. Bodek and J. L. Ritchie, *Phys. Rev. D* **23**, 1070 (1981).
- [32] D. Rein and L. M. Sehgal, *Ann. Phys. (N.Y.)* **133**, 79 (1981).
- [33] A. Bodek, I. Park, and U. Yang, *Nucl. Phys. B, Proc. Suppl.* **139**, 113 (2005).
- [34] T. Yang, C. Andreopoulos, H. Gallagher, K. Hoffman, and P. Kehayias, *Eur. Phys. J. C* **63**, 1 (2009).
- [35] K. Abe *et al.* (T2K Collaboration), *Phys. Rev. D* **87**, 092003 (2013).
- [36] FGD1 also contains hydrogen. Pure diffractive scattering from the protons can occur that, at low Q^2 , may result in a similar final state to that produced by coherent interactions on nuclei. The contribution of diffractive scattering from hydrogen to the selected event sample was estimated to be less than 5%.
- [37] A photon equivalent unit is a measure of the response of the FGD to single photons. A single PEU corresponds to a deposited energy of 0.046 MeV.
- [38] P. Rodrigues, C. Wilkinson, and K. McFarland, *Eur. Phys. J. C* **76**, 474 (2016).
- [39] D. Ashery, I. Navon, G. Azuelos, H. K. Walter, H. J. Pfeiffer, and F. W. Schlepütz, *Phys. Rev. C* **23**, 2173 (1981).
- [40] M. Martini, M. Ericson, G. Chanfray, and J. Marteau, *Phys. Rev. C* **81**, 045502 (2010).
- [41] J. Nieves, M. Valverde, and M. J. VicenteVacas, *Phys. Rev. C* **73**, 025504 (2006).
- [42] G. A. Fiorentini *et al.* (MINERvA Collaboration), *Phys. Rev. Lett.* **111**, 022502 (2013).
- [43] P. A. Rodrigues *et al.* (MINERvA Collaboration), *Phys. Rev. Lett.* **116**, 071802 (2016).
- [44] K. Abe *et al.* (T2K Collaboration), *Phys. Rev. D* **88**, 032002 (2013).